Breast Cancer Res Treat (2009) 115:523–535
DOI 10.1007/s10549-008-0094-2

PRECLINICAL STUDY

Association between farnesoid X receptor expression and cell proliferation in estrogen receptor-positive luminal-like breast cancer from postmenopausal patients

Fabrice Journe · Virginie Durbecq · Carole Chaboteaux · Ghizlane Rouas · Guy Laurent · Denis Nonclercq · Christos Sotiriou · Jean-Jacques Body · Denis Larsimont

Received: 31 March 2008 / Accepted: 5 June 2008 / Published online: 19 June 2008

Abstract The farnesoid X receptor (FXR, NR1H4), a member of the nuclear receptor superfamily of ligand-dependent transcription factors, is normally produced in the liver and the gastrointestinal tract, where it acts as a bile acid sensor. It has been recently detected in breast cancer cell lines and tissue specimens. The expression of FXR was scored (0–8) by immunohistochemistry on 204 breast cancer samples and correlated with established cancer biomarkers. Moreover, the effect of the FXR activator chenodeoxycholic acid (CDCA) was determined on cell proliferation and estrogen receptor regulation/activation in breast cancer cell lines. FXR was detected in 82.4% of samples with a high median expression score of 5. FXR expression significantly correlated with estrogen receptor (ER) expression ($P = 0.009$) and luminal-like markers. In ER-positive tumors, FXR expression was significantly correlated with the proliferation marker Ki-67 ($P < 0.001$) and the nodal status ($P = 0.028$), but only so in post-menopausal women, suggesting that lack of estrogens may disclose the association between FXR and cell proliferation. In vitro experiments confirmed clinical data since CDCA stimulated the proliferation of ER-positive cells only in steroid-free medium, a stimulation inhibited upon siRNA-silencing of FXR expression as well as ER blockade by antiestrogens. Moreover, co-immunoprecipitation experiments revealed that CDCA activated-FXR interacted with ER. These results suggest that ER-positive breast tumors could be stimulated to proliferate via a crosstalk between FXR and ER, particularly in a state of estrogen deprivation (menopause, aromatase inhibitors).

Keywords NR1H4 · Breast cancer · Estrogen receptor · Ki-67 · Immunohistochemistry · Bile acids

Fabrice Journe and Virginie Durbecq had contributed equally to this work and should be considered as joint first authors.

F. Journe · V. Durbecq · C. Chaboteaux · G. Rouas · C. Sotiriou · J.-J. Body · D. Larsimont
Laboratory of Endocrinology & Translational Research Unit, Department of Internal Medicine, Institut Jules Bordet, Université Libre de Bruxelles (ULB), Brussels, Belgium

F. Journe (✉)
Laboratory of Endocrinology and Bone Diseases, Institut Jules Bordet, Université Libre de Bruxelles (ULB), 1 rue Héger-Bordet, 1000 Brussels, Belgium
e-mail: fabrice.journe@bordet.be

G. Laurent · D. Nonclercq
Laboratory of Histology, Faculty of Medicine and Pharmacy, Université de Mons-Hainaut (UMH), Mons, Belgium

Introduction

The farnesoid X receptor (FXR, NR1H4) was initially isolated in 1995 as an orphan nuclear receptor activated by farnesol, a metabolic intermediate of the mevalonate pathway [1]. In subsequent studies, FXR was deorphanized by the identification of bile acids (in particular chenodeoxycholic acid, CDCA) as cognate ligands [2–4]. Presently, FXR is considered as a member of the metabolic nuclear receptor family [5]. Like other nuclear receptors, it functions as a ligand-activated transcription factor. Thus it contains a DNA binding domain capable of interacting with specific *cis*-DNA sequences (FXR response elements, FXRE's) associated with the promoters of target genes. It also exhibits a ligand binding domain accepting small lipophilic molecules [6]. Upon ligand-induced activation, FXR generally heterodimerizes with the retinoid X receptor (RXR) and binds to inverted repeat-1 motifs (IR-1) or other motifs present in FXRE's [7].

In early studies, FXR was shown to exhibit a rather narrow tissue distribution, its expression being restricted to the liver, the intestine, the kidney and the adrenal gland [1]. In the liver and the gastrointestinal tract, it functions as a bile acid sensor and regulates bile acid homeostasis, lipid and glucose metabolism, and hepatic regeneration [6]. In hepatocytes, it indirectly inhibits the cytochrome p450 enzyme cholesterol 7-α-hydroxylase (CYP7A1) involved in the conversion of cholesterol into bile acids, and it induces the synthesis of a variety of proteins implicated in the metabolism and transport of lipids [7, 8]. Thus, FXR has emerged as a new therapeutic target for the management of lipid disorders [9, 10].

In addition, FXR has recently been detected in vascular smooth muscle cells [11] and endothelial cells [12]. Surprisingly, we and others have also found FXR expression in breast cancer tissue and breast cancer cell lines [13–15]. With regard to breast cancer development, the presence of high plasma levels of deoxycholic acid in postmenopausal breast cancer patients, as compared to healthy controls matched for age and body mass index, has been documented, suggesting that this bile acid might be involved in mammary gland carcinogenesis [16]. Moreover, accumulation of bile acids from serum has been reported in breast cyst fluid and has been discussed as a potential risk factor for developing breast cancer [17–19]. Strikingly, recent data from our group reveal a positive crosstalk between FXR and estrogen receptor alpha (henceforth abbreviated as ER), accounting for FXR-mediated ER activation in absence of estrogens and resulting in a mitogenic response of breast carcinoma cells to farnesol [15].

In this retrospective study, we assessed by immunohistochemistry FXR expression in breast cancer tissue specimens and we analyzed its correlation with classical breast cancer biomarkers in order to evaluate the FXR prognostic significance in breast cancer. Furthermore, we determined the effects of FXR activation by bile acid in breast cancer cell lines grown in steroid-free medium supplemented or not with estrogen.

Materials and methods

Breast cancer tissue sampling

Formalin-fixed, paraffin-embedded primary breast cancer samples collected from 204 patients at the Institut Jules Bordet were used for the evaluation of FXR expression. Patients with primary invasive breast cancer were included in the study, while patients with bilateral breast cancer as well as previous or concomitant cancer other than breast cancer were excluded. All marker analyses were performed on breast cancer tissue specimens collected in patients who did not receive neoadjuvant therapy. A subpopulation of 120 untreated breast cancer patients was selected to evaluate the "pure" prognostic value of FXR. The study was performed according to the REMARK recommendations from the National Cancer Institute—European Organisation for Research and Treatment Cancer [20].

The clinico-pathological characteristics of the population are described in Table 1. Objective assessment of FXR and other biomarkers was performed by immunohistochemical analysis of tissue microarrays (TMA). Thus, representative core needle specimens (0.6 mm diameter) of invasive cancer tissue (identified as such by histological examination of hematoxylin/eosin-stained sections) were punched from donor tissue blocks and transferred to recipient blocks using a specific arraying device (Beecher Instruments Silver Spring, MD, USA). A minimum of 4 tissue cores was taken per donor tissue block to minimize the problem of tumor heterogeneity. The ethics committee of the Institute approved the use of the tissue material for this study.

Immunohistochemical evaluation of FXR expression

TMA blocks were cut and tissue sections were mounted on poly-L-Lysine-coated glass slides. Immunohistochemical staining was performed with an antibody raised against human FXR (mouse monoclonal anti-human FXR/NR1H4 antibody, clone A9033A, R&D Systems, Minneapolis, MN, USA). Prior to immunostaining, antigen retrieval was achieved by microwave pretreatment (2 × 10 min at a power of 650 W) in citrate buffer pH 6.0. Thereafter, tissue sections were incubated for 30 min at 37°C in presence of the primary antibody diluted 1:25. FXR antigen–antibody reaction was visualized using Ventana automated system with the highly sensitive Nexes reagents (Enhanced Nexes reagent, Ventana Medical Systems, Tucson, AZ, USA). Nuclear staining was defined as positivity. FXR expression was scored from 0 to 8 by adding a score reflecting the proportion of positively stained cells (none: 0, <1/100: 1, 1/100 to 1/10: 2, 1/10 to 1/3: 3, 1/3 to 2/3: 4 and >2/3: 5) and a score reflecting the staining intensity (none: 0, weak: 1, intermediate: 2 and strong: 3), as defined by Allred et al. [21]. The semi-quantitative analysis was performed in a single-blind fashion by an experienced pathologist (D.L.).

Other antibodies used for immunohistochemistry were raised against estrogen receptor (ER, clone 6F11), progesterone receptor (PgR, clone AB), HER-2/neu (clone CB11), p27 (clone 1B4), c-myc (clone 9E11), mucin-1 (muc-1, clone Ma552) and cytokeratins 8/18 (CK8/18, clone 5D3) (from Novocastra, Newcastle upon Tyne, UK); Ki-67 (clone MIB1), epidermal growth factor receptor (EGFR, kit), CK5/6 (clone D5/6B4) (from Dako Belgium, Heverlee, Belgium); GATA-3 (clone HG3-31) and cyclin E

Table 1 Clinico-pathological characteristics of the study population

	Total population $n = 204$	ER+ population $n = 109$	ER− population $n = 59$
Median age, years (range)	57 (26–93)	59 (30–93)	54 (34–83)
Menopausal status (>50 years)	139/204 (68.1%)	83/109 (76.1%)	33/59 (55.9%)
ER positive	109/168 (64.9%)		
PgR positive	88/167 (52.7%)	72/108 (66.7%)	16/59 (27.1%)
Node positive	33/182 (18.13%)	12/103 (11.65%)	9/59 (15.25%)
Histological grade			
Grade 1	39/170 (22.9%)	26/101 (24.7%)	10/51 (19.6%)
Grade 2	91/170 (53.5%)	57/101 (56.4%)	21/51 (41.2%)
Grade 3	40/170 (23.5%)	18/101 (17.8%)	20/51 (39.2%)
HER-2/neu (score 2 or 3)	27/204 (13.2%)	7/109 (6.4%)	12/59 (20.3%)
Ki-67			
Median	5%	5%	5.25%
>25%	18/164 (11%)	8/106 (7.5%)	10/58 (17.2%)
Non evolutive primary breast cancer	92/166 (55.4%)	60/79 (75.9%)	32/53 (60.4%)
Evolutive primary breast cancer	74/166 (44.6%)	19/79 (24.1%)	21/53 (39.6%)

(clone He12) (from Santa Cruz Biotechnology, Santa Cruz, CA, USA); cyclin D (P2D11F11) (from Ventana Medical System); AIB-1 (clone 34) (from BD Biosciences, Erembodegem, Belgium) and topoisomerase II alpha (Topo II, clone KiS1) (from Chemicon, Temecula, CA, USA). All markers were scored from 0 to 8, except Ki-67 and Topo II for which the percentages of positively stained cells were reported, and HER-2/neu for which the expression was scored from 0 to 3 (scoring system recommended for the Dako Hercep Test, Carpinteria, CA, USA). Biomarker overexpression was defined as a Topo II score >10%, a HER-2/neu score of 3, and a scoring ≥2 for all other biomarkers. Samples with a Ki-67>25% were considered as highly proliferating tumors.

Breast cancer cell lines and culture conditions

The ER-positive MCF-7 breast cancer cell line (ATCC HTB-22) and the ER-negative MDA-MB-231 breast carcinoma cell line (ATCC HTB-26) were both obtained from the American Type Culture Collection (Manassas, VA, USA). Cells were cultured at 37°C in a humidified 95% air and 5% CO_2 atmosphere. For routine maintenance, cells were propagated in 75-cm^2 flasks containing Eagle's Minimum Essential Medium (MEM) with Phenol Red, supplemented with 10% heat-inactivated fetal bovine serum (FBS) and with L-glutamine, penicillin and streptomycin (Gibco BRL, Life Technologies, Merelbeke, Belgium) at standard concentrations. Cells were harvested by trypsinization (0.1% trypsin–0.02% EDTA) and subcultured twice weekly. For experiments, cells were plated in steroid-free medium (SFM) consisting of MEM without Phenol Red supplemented with 10% dextran-coated charcoal-treated FBS to suppress potential influence of serum-derived lipid compounds. One or two days after seeding, the culture medium was replaced by fresh SFM containing chenodeoxycholic acid (CDCA, Sigma, St Louis, MO, USA), 17β-estradiol (E_2, Sigma), 4-hydroxytamoxifen (tamoxifen, Sigma), fulvestrant (ICI 182,780, Tocris, Bristol, UK), or vehicle (control). Cells were treated for 10–60 min or 1–3 days, with drugs alone or in combinations, as specified in "Results".

Western blot analysis

Cells were plated in 60-cm^2 Petri dishes (5×10^5 cells per dish) containing SFM. Two days after seeding, cells were cultured for 24 h in fresh SFM containing 50 μM CDCA, 1 nM 17β-estradiol, 100 nM 4-hydroxytamoxifen, 100 nM fulvestrant, or vehicle (control), alone or in combinations as specified in "Results". Then, cells were lysed using detergent cocktail, as previously described [15]. Protein concentrations were determined by the BCA Protein Assay (Pierce, Rockford, IL, USA) using bovine serum albumin as standard. Equal amounts of cell proteins or 10 ng recombinant FXR protein (rFXR, Active Motif, Rixensart, Belgium) were subjected to Western blotting using a rabbit polyclonal anti-human FXR/NR1H4 antibody (Abcam, Cambridge, UK) diluted 1:1000, a mouse monoclonal anti-human ERα antibody (F-10, Santa Cruz Biotechnology) diluted 1:5,000, a mouse monoclonal anti-human PgR (A/B isoforms) antibody (NCL-PGR-AB, Novocastra) diluted 1:500, a mouse monoclonal anti-human cyclin D1 antibody (DCS6, Cell Signaling Technology, Beverly, MA, USA)

diluted 1:2,000, or a rabbit polyclonal anti-mouse p27 antibody (Cell Signaling Technology) diluted 1:1000. β-actin was used as a loading control, and was demonstrated with a mouse monoclonal anti-human actin antibody (Chemicon) diluted 1:7,500. Of note, neutralization of the rabbit polyclonal anti-human FXR/NR1H4 antibody with excess rFXR (incubation for 2 h at room temperature) was used to document the specificity of the antibody. Peroxidase-labeled anti-rabbit IgG antibody (1:10,000) or peroxidase-labeled anti-mouse IgG antibody (1:10,000) (Amersham Pharmacia Biotech, Roosendaal, The Netherlands) were used as secondary reagents to detect corresponding primary antibodies. Bound peroxidase activity was revealed using the SuperSignal® West Pico Chemiluminescent Substrate (Pierce). Immunostaining signals were digitalized with a PC-driven LAS-3000 CCD camera (Fujifilm, Tokyo, Japan), using a software specifically designed for image acquisition (Image Reader, Raytest®, Straubenhardt, Germany). Immunoreactive band intensities were quantified using the software AIDA® Image Analyser 3.45 (Raytest®).

Receptor co-immunoprecipitation

The formation of FXR/ER complexes in cells exposed to CDCA was determined by co-immunoprecipitation experiments, using first an anti-FXR antibody to immunoprecipitate FXR, followed by an anti-ER antibody to demonstrate by Western blotting the presence of ER in the immunoprecipitates. MCF-7 cells were plated in 60-cm^2 Petri dishes (10^6 cells per dish) in SFM and cultured for 24 h. Control cells were not incubated further, while treated cells were exposed to 50 μM CDCA for 10, 20, 30 and 60 min as indicated in "Results". Cell monolayers were rinsed, harvested and lysed using detergent cocktail, as described in "Western blot analysis" section. Clarified supernatants containing equivalent amounts of proteins (1 mg), as determined by the BCA Protein Assay, were diluted with lysis buffer up to 500 μl; aliquots were saved for total FXR and ER expression determinations (see "Western blot analysis"). In order to remove proteins that may otherwise cross react at the time of immunoprecipitation, supernatants were incubated with 100 μl of anti-rabbit IgG antibody-agarose (Sigma) for 2 h under agitation, and then centrifuged. Supernatants were therefore incubated overnight with the rabbit polyclonal anti-human FXR/NR1H4 antibody (Abcam) diluted 1:100. FXR-antibody complexes were precipitated with 100 μl of anti-rabbit IgG antibody-agarose for 2 h under agitation, and collected by centrifugation. Pellets were washed four times with the lysis buffer (see "Western blot analysis"), suspended in 60 μl electrophoresis sample buffer, and boiled for 5 min. Samples were finally subjected to Western blotting to assess ER levels, using the mouse monoclonal anti-human ERα antibody F-10, as described above. Non specific interactions were evaluated by omitting the anti-FXR antibody during the immunoprecipitation process.

Immunofluorescence microscopy

Cells were plated in SFM on sterile round glass coverslips in 12-well dishes, and cultured for 3 days without any treatment or cultured for 2 days and exposed to 50 μM CDCA or vehicle for additional 24 h. Cell monolayers were fixed with paraformaldehyde (PAF) and processed for immunofluorescence staining as described previously [15]. Mouse monoclonal anti-FXR/NR1H4 antibody (clone A9033A, R&D Systems) or rabbit polyclonal anti-ER antibody (HC-20, Santa Cruz Biotechnology) were used as primary reagents (dilution 1:50). The cell preparations were subsequently, and in succession, exposed to a dextran polymer coated with both peroxidase and antibodies raised against mouse or rabbit immunoglobulins (EnVision™, Dako Belgium), rabbit anti-peroxidase antiserum (Laboratory of Hormonology, Marloie, Belgium), biotinylated swine anti-rabbit immunoglobulins antibodies (Dako Belgium) and Texas Red-conjugated streptavidin (Vector Laboratories, Burlingame, CA, USA). The coverslips were mounted on glass slides using commercial anti-fading medium (Vectashield®, Vector Laboratories). The cell preparations were examined on a Leitz Orthoplan microscope equipped with a Ploem system for epi-illumination. Excitation wavelength of 560 nm and emission wavelength of 590 nm were used for the observation of Texas Red fluorescence. The appearance of immunostained cell preparations was documented by using a PC-driven digital camera (Leica DC 300F, Leica Microsystems AG, Heerbrugg, Switzerland). Microscopic fields were digitalized and stored thanks to a software specifically designed for image acquisition (Leica IM 50, Leica Microsystems AG).

Crystal violet growth assay

Cell number was assessed indirectly by staining with crystal violet dye as previously described [15]. Briefly, cells were seeded in 96-well plates (10^3 cells per well) in SFM supplemented or not with 1 nM 17β-estradiol, and cultured for 24 h. Cells were then exposed to 1-200 μM CDCA or vehicle (control) for 3 days. After medium removal, cells were gently washed with PBS, fixed with glutaraldehyde/PBS and stained with crystal violet. Cells were destained under running tap water and subsequently lysed with Triton X-100. The absorbance was measured at 550 nm using a Microplate Autoreader EL309 (BIO-TEK Instruments, Winooski, VT, USA). Blank wells were used

for background subtraction and untreated cell cultures were run in parallel as controls.

Gene silencing with small interfering RNA (siRNA)

The siRNA targeting the human FXR with the cDNA sequence 5′-GAGGAUGCCUCAGGAAAUA-3′ was synthesized and annealed by Eurogentec (Seraing, Belgium). The siRNA duplex negative control (scramble; cDNA sequence 5′-AAAGCGUCUGGAAAAGUCG-3′) from Eurogentec was used to evaluate the non-specific effects on transfection on gene expression. MCF-7 cells (10^6 cells in 60-cm^2 Petri dishes) were cultured in SFM for 16 h and transfected for 6 h with 50 nM siRNA duplex using jetSI-ENDO (Eurogentec) in OptiMEM (Gibco BRL, Life Technologies, Merelbeke, Belgium) or vehicle (mock) according to the manufacturer's instructions. Transfected cells were fed fresh SFM and further cultured for 16 h. A pool of transfected cells was harvested by trypsinization, plated in 96-well plates (10^3 cells per well), cultured for 24 h, and then exposed to 50 μM CDCA or vehicle for 3 days to assess cell proliferation (crystal violet growth assay). In parallel, another pool of transfected cells (mock, siRNA FXR and scramble) was further cultured for 24 h before determination of FXR and ER expressions (Western blot analysis).

Statistical analysis

All statistical analyses were performed using SPSS 15.0 Inc. (Chicago, IL, USA). Correlations between FXR expression—as evaluated by immunohistochemistry—and pathological parameters were determined through the calculation of non-parametric Spearman's rank correlation coefficients. Association between parameters was assessed using the concordance coefficient Kappa (for binary variables) and Mann-Whitney tests (FXR expression as a function of ER status). To perform the analyses, dichotomized immunohistochemical data were used for tumour grade and size, FXR and Ki-67 expression as well as patient's age and nodal status: tumor grade 1 or 2 vs. 3, tumor size $\leq$2 cm vs. >2 cm, FXR score <2 vs. $\geq$2, Ki-67 $\leq$25% vs. >25%, age $\leq$50 years vs. >50 years (=menopausal status), and node negative vs. node positive. Distant metastasis-free survival was defined as the interval elapsed between the time of surgery and the diagnostic of distant metastasis. P-values < 0.05 were considered as statistically significant. In vitro data are reported as means $\pm$ SD and statistical analysis was performed by analysis of variance (ANOVA). Dunnett post hoc test was used to compare treated conditions to the untreated condition (control) and Tukey post hoc test was performed for multiple comparisons between groups. For in vitro studies, the level of statistical significance was arbitrarily set at 0.01.

Results

Evaluation of FXR expression in breast cancer cell lines and tissue specimens

In preliminary experiments, primary antibodies used in this study for FXR detection by Western blotting (rabbit polyclonal anti-FXR antibody) and immunofluorescence/immunohistochemistry (mouse monoclonal anti-FXR antibody, clone A9033A) were tested with regard to immunoreactivity and specificity. Results are illustrated in Fig. 1 and 2.

Immunoblot analysis of human recombinant FXR (rFXR) with the polyclonal antibody detected an immunoreactive band at the expected molecular mass for FXR (60 kDa) (Fig. 1a). Furthermore, a drastic reduction in band density was observed when the antibody was preincubated with the rFXR protein. Immunoblot analysis of lysates from ER-positive MCF-7 and ER-negative MDA-MB-231 breast carcinoma cells revealed the presence of similar 60 kDa immunoreactive bands (Fig. 1a), which disappeared when the neutralized anti-FXR antibody was used.

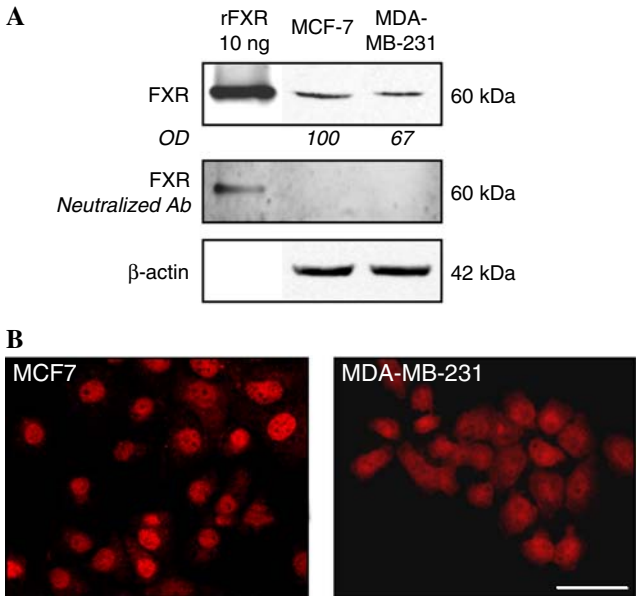

Fig. 1 FXR expression in breast cancer cell lines. (**a**) FXR was assessed in MCF-7 and MDA-MB-231 cells by Western blotting with a rabbit polyclonal anti-FXR/NR1H4 antibody. The specificity of the signal was proved by the immunodetection of a recombinant FXR protein (rFXR), and the significant reduction of the signal by using rFXR-neutralized antibody. β-actin was used as a loading control. Quantitative data were obtained from densitometric analyses ($n = 2$) and are presented as mean percentages. (**b**) Demonstration of FXR in MCF-7 and MDA-MB-231 cell lines by immunofluorescence microscopy with a mouse monoclonal anti-FXR/NR1H4 antibody. Texas Red labeling. Magnification bar: 10 μm

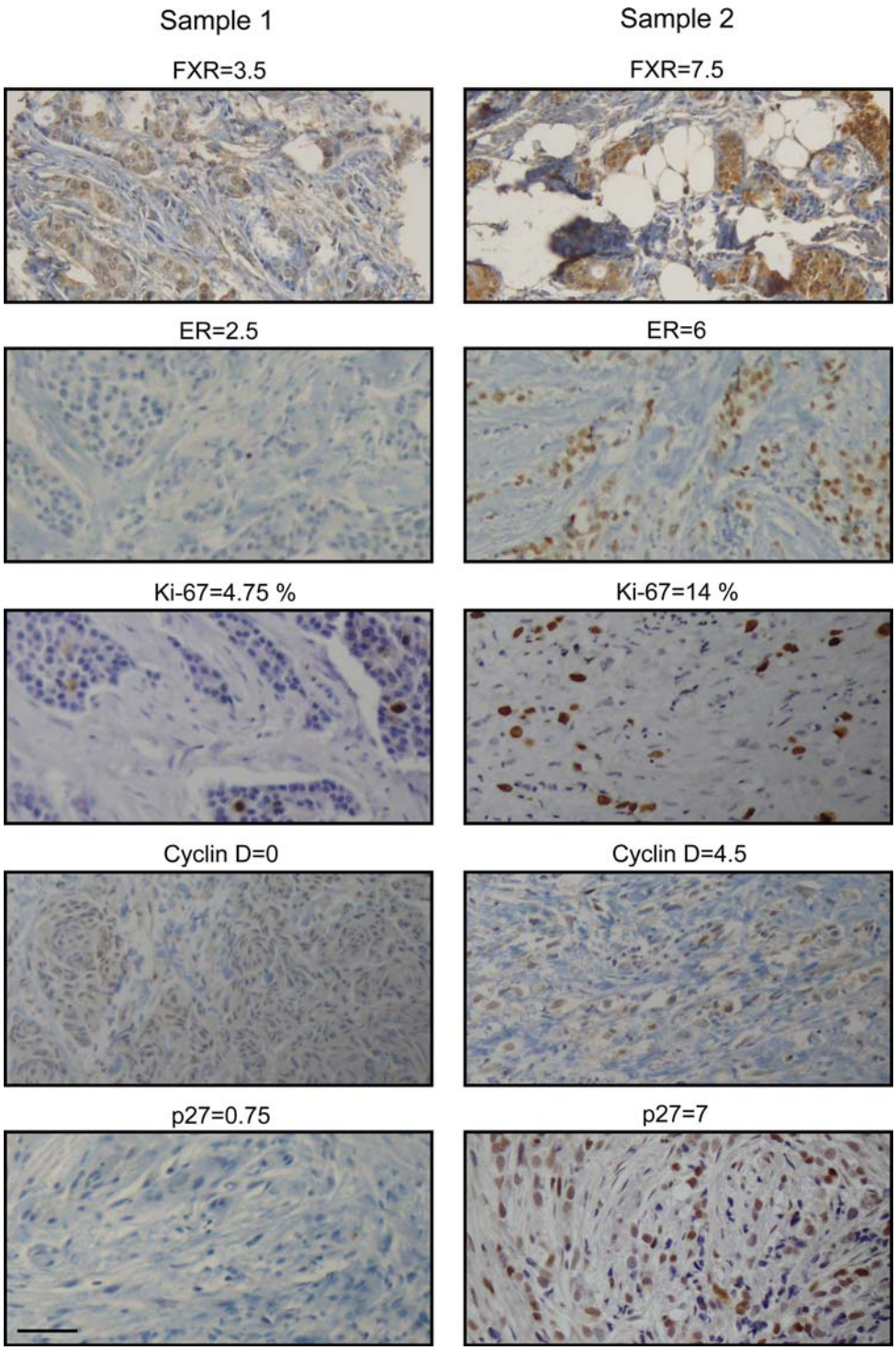

Fig. 2 Expression of FXR and biomarkers in human breast cancer tissue specimens. Cancer samples were subjected to immunohistochemical analysis with different antibodies as described in "Materials and Methods". Representative data of low/moderate FXR expression (sample 1) and of high FXR expression (sample 2) in ER-positive breast cancer tissue. FXR expression clearly correlates with that of ER, Ki-67, cyclin D and p27. Magnification bar: 50 μm

The rabbit polyclonal anti-FXR antibody did not give satisfactory results when used for immunofluorescence microscopy and immunohistochemistry (data not shown). By contrast, mouse monoclonal anti-FXR antibody demonstrated the presence of FXR immunoreactivity in nuclei of both MCF-7 and MDA-MB-231 cells (Fig. 1b). Thus, the latter antibody was used for FXR immunostaining in clinical breast tumor specimens (Fig. 2).

FXR expression in ER-positive and ER-negative breast cancer tissue specimens

FXR expression was assessed by immunohistochemistry in 204 breast cancer samples, along with a panel of biomarkers routinely used for the immunohistochemical characterization of breast carcinoma [22]. These samples were representative of a typical breast cancer population,

insofar as ER expression was present in 2/3 of cases, HER-2/neu receptor expression was present in nearly 15% of cases, histological grade 1 and grade 3 samples represented each one 1/4 of the population, and 80% of the samples originated from node negative patients (Table 1).

Representative microscopic fields in Fig. 2 illustrate FXR immunostaining in tissue specimens from two breast tumor cases with low/moderate (sample 1, left column) and high (sample 2, right column) expressions of the FXR protein. In the whole population, FXR was detected (median score = 5) in 82.4% of the samples (Table 2). Interestingly, a significantly higher FXR expression was detected in the ER-positive subgroup (median score = 6) than in the ER-negative one (median score = 4). These data are in agreement with the observations on breast cancer cell lines showing that FXR is expressed at a higher level in ER-positive MCF-7 cells, as compared to ER-negative MDA-MB-231 cells (Fig. 1).

In the total population, significant correlations (Spearman's rho) were observed between the expression of FXR and that of steroid hormone receptors (ER and PgR), and between FXR and the proliferation marker Ki-67 (Table 2) (typical cases illustrated in Fig. 2). FXR expression also correlated with Ki-67 and the nodal status in the ER-positive subgroup while no significant correlation between FXR and other biomarkers was detected in the ER-negative subgroup (Table 2). Nevertheless, in the ER-positive subgroup, no relationship was observed between FXR and the tumor histological grade.

FXR expression in ER-positive breast cancers according to menopausal status of patients

In the ER-positive population, we found a weak correlation between FXR expression and the patients' age at diagnosis in the premenopausal but not in postmenopausal patients (Table 3). These data suggest that FXR expression increases with age to reach a maximum in tumors from postmenopausal patients.

Moreover, an analysis of the ER-positive population revealed that the statistically significant associations between FXR expression and Ki-67 expression ($P = 0.017$), and between FXR expression and the patients' nodal status ($P = 0.029$) were documented only in the postmenopausal women (Table 3). These data suggest that the lack of estrogens related to menopause may disclose the correlation between FXR expression and cellular proliferation in the ER-positive tumors.

Prognostic importance of FXR expression in ER-positive tumors

To assess the prognostic value of FXR with regard to distant metastasis-free survival, FXR evaluation was performed on 120 node-negative breast cancer patients from Institut Jules Bordet. We selected patients who underwent breast cancer surgery between 1987 and 1989 and did not receive systemic adjuvant therapy, and for whom a median follow-up of 10 years (range 2–16 years) was available (Table 4).

FXR expression was significantly correlated with ER and PgR, the transcription factor GATA-3 and the ER coactivator AIB-1, indicating a close association between FXR expression and the hormone-responsive phenotype. FXR expression was also correlated with CK8/18 and muc-1, supporting further association with the ER-positive luminal-like breast cancer subtype (Table 4).

As previously reported for the total patient population described in Table 1, FXR expression was significantly

Table 2 Association of FXR expression with pathological markers according to ER status

	FXR score Total population	FXR score ER+ subgroup	FXR score ER− subgroup
FXR			
Median score	5	6*	4*
Positivity	168/204 (82.4%)	94/109 (86.2%)**	44/59 (74.6%)**
Age at diagnosis	0.009[a]; ns[b] (204)[c]	0.004; ns (109)	−0.135; ns (59)
Histological grade	−0.059; ns (185)	−0.007; ns (108)	0.004; ns (59)
Menopausal status (<50 vs. >50)	0.043; ns (204)	0.019; ns (109)	0.091; ns (59)
Metastasis	−0.090; ns (166)	−0.028; ns (79)	−0.014; ns (53)
ER score	**0.228; 0.009 (129)**		
PgR score	**0.202; 0.021 (129)**	0.206; ns (77)	0.070; ns (52)
Ki67%	**0.288; <0.001 (164)**	**0.385; <0.001 (106)**	0.181; ns (58)
Tumor size	−0.159; ns (173)	−0.142; ns (102)	0.072; ns (50)
Nodal status	0.054; ns (182)	**0.228; 0.020 (103)**	0.097; ns (59)

* Mann–Whitney test, $P < 0.001$; ** Kappa test, $P = 0.060$

[a] Correlation coefficient (Spearman's rho); [b] Significance; ns = No significant; [c] Number of cases. Bold text indicates statistically significant associations

Table 3 Association of FXR expression with pathological markers in ER-positive tumors according to menopausal status

	FXR score ≤50 Years old, ER+ subgroup	FXR score >50 Years old, ER+ subgroup
FXR		
Median score	6*	6*
Positivity	24/26 (92.3%)**	70/83 (84.3%)**
Age at diagnosis	**0.396**[a]; **0.044**[b] **(26)**[c]	−0.053; ns (83)
Histological grade	−0.079; ns (26)	0.027; ns (82)
Metastasis	−0.326; ns (18)	0.057; ns (61)
PgR score	0.403; ns (18)	0.192; ns (59)
Ki67%	0.237; ns (26)	**0.454**; **<0.001 (80)**
Tumor size	0.086; ns (26)	−0.226; ns (76)
Nodal status	0.201; ns (26)	**0.251**; **0.028 (77)**

* Mann–Whitney test, $P = 0.843$; ** Kappa test, $P = 0.303$

[a] Correlation coefficient (Spearman's rho);
[b] Significance; ns = No significant; [c] Number of cases. Bold text indicates statistically significant associations

correlated with the proliferation marker Ki-67 as well as with several other proliferation markers including Topo II, c-myc transcription factor, and especially cyclin D and p27 protein. FXR expression still showed a strong correlation with cyclin D and p27 in the ER-positive breast cancer subgroup of good prognosis (follow-up >10 years), while its expression was correlated only with the proliferation marker c-myc in the ER-positive subgroup of poor prognosis (Table 4). In agreement with the fact that FXR expression was similar in the tumors of good and poor prognosis patients, no association was observed between FXR expression and the risk of cancer recurrence in the total population or in the ER-positive subgroup (data not shown).

Effect of FXR activation on cell proliferation and biomarker expression: in vitro data

The findings outlined above prompted us to examine the effect of the primary bile acid chenodeoxycholic acid (CDCA), the most potent endogenous ligand/activator of FXR [4], on the proliferation of MCF-7 and MDA-MB-231 cells cultured in steroid-free medium (SFM) supplemented or not with estrogen (Fig. 3a). In estrogen-supplemented medium, CDCA had no effect, while it stimulated the proliferation of the ER-positive MCF-7 cells in SFM. In agreement with the lack of correlation between FXR and Ki-67 observed in ER-negative tumor specimens, CDCA had no mitogenic action on the ER-negative MDA-MB-231 cells, regardless of the culture conditions. Of note, as reported by another group [14], bile acid concentrations over 100 μM were toxic for breast cancer cells. The specific involvement of FXR in the proliferative response of MCF-7 cells to CDCA was checked by silencing the expression of the receptor with an anti-FXR siRNA. As shown in Fig. 3b, FXR expression silencing by the siRNA partly suppressed the proliferative response of MCF-7 cells to CDCA, while a scramble RNA was inactive. Of note, siRNA against FXR did not affect ER expression in MCF-7 cells, confirming the specificity of the siRNA.

Previous work of our group has disclosed the existence of a crosstalk between FXR and ER in breast carcinoma cells [15]. Thus, as illustrated in Fig. 3c, the mitogenic action of CDCA on MCF-7 cells was abrogated by the antiestrogens 4-hydroxytamoxifen and fulvestrant (ICI 182,780). As expected, antiestrogens did not alter FXR expression in MCF-7 cells. In addition, co-immunoprecipitation experiments revealed that FXR interacts with ER when activated by CDCA (Fig. 4). As a consequence of such interactions, FXR activation by CDCA results in typical estrogenic responses, i.e. ER downregulation and induction of the progesterone receptor (PgR) (Fig. 5).

In addition, as illustrated in Fig. 5a, CDCA and E_2 exerted opposite effects on the cdk inhibitor p27, whereas these drugs induced an increase of the cell cycle mediator cyclin D1, suggesting that they somehow differ in their action on G1 phase progression. Results obtained here with E_2 are consistent with previous work showing that MCF-7 cell exposure to estrogen leads to a decrease of p27 [23] due to enhanced proteasomal degradation [24], and a concomitant activation of cyclin E-cdk2. On the other hand, the fact that CDCA induces both a proliferative response (Fig. 3) and an increase of p27 (Fig. 5) was in agreement with in vivo data and suggests that the latter cdk inhibitor accumulates in an inactive form or is prevented from exerting an inhibitory effect on cyclin E-cdk2. Cyclin D1-cdk4 complexes might titrate p27 away from cyclin E-cdk2 complexes, allowing these complexes to become active [25].

Overall, observations performed in vitro match in vivo findings since they confirm the relationship between FXR expression/activation, ER expression/activation and enhanced cell proliferation.

Discussion

The nuclear receptor FXR has been recently demonstrated in breast cancer as well as in normal mammary tissue [13–15]. The present study reveals a higher FXR

Table 4 Association of FXR expression with pathological markers in ER-positive population according to prognosis

	FXR score Total population	FXR score ER+ population, good prognosis (no metastasis in 10 years of follow-up)	FXR score ER+ population, poor prognosis (distant metastasis)
FXR			
Median score	5	5.5*	5.25*
Positivity	93/120 (77.5%)	49/60 (81.7%)**	11/14 (78.6%)**
Hormone-responsive markers			
ER score	**0.289**[a]; **0.001**[b] **(120)**[c]		0.245; ns (13)
GATA-3 score	**0.514**; **<0.001 (118)**	**0.393**; **0.002 (59)**	−0.178; ns (12)
AIB-1 score	**0.408**; **<0.001 (115)**	**0.399**; **0.002 (59)**	0.333; ns (14)
PgR score	**0.247**; **0.006 (120)**	0.213; ns (60)	
Luminal subtype markers			
CK8/18	**0.252**; **0.005 (120)**	0.205; ns (60)	0.039; ns (14)
CK5/6	−0.064; ns (120)	−0.103; ns (60)	no data
Muc-1	**0.207; 0.023 (119)**	0.170; ns (60)	−0.370; ns (14)
Proliferative markers			
Ki67 %	**0.245**; **0.007 (118)**	0.249; ns (58)	0.468; ns (14)
Topo II %	**0.208**; **0.022 (120)**	**0.267**; **0.038 (60)**	0.338; ns (14)
Cyclin D score	**0.498**; **<0.001 (118)**	**0.513**; **<0.001 (58)**	0.493; ns (14)
Cyclin E score	0.004; ns (120)	**0.259**; **0.045 (60)**	−0.018; ns (14)
c-myc Score	**0.278; 0.002 (119)**	**0.254; 0.049 (60)**	**0.653; 0.015 (13)**
p27 Score	**0.553; <0.001 (119)**	**0.467; <0.001 (60)**	0.469; ns (14)
neu Score	−0.059; ns (120)	0.007; ns (60)	no data
EGFR score	−0.082; ns (120)	no data	−0.069; ns (14)

* Mann–Whitney test, $P = 0.799$; ** Kappa test, $P = 0.800$

[a] Correlation coefficient (Spearman's rho); [b] Significance; ns = No significant; [c] Number of cases. Bold text indicates statistically significant associations

expression in ER-positive luminal-like tumors, as compared to ER-negative breast tumors. These data are consistent with the semi-quantitative analysis of FXR in the ER-positive cell line MCF-7 and the ER-negative cell line MDA-MB-231 and support the hypothesis of a lower FXR expression in less differentiated tumor cells (such as ER-negative breast carcinoma cells). Similar observations have been made in other malignancies. Indeed, FXR mRNA levels decrease in colon adenomas and even more in colon carcinomas, and become undetectable in undifferentiated colon adenocarcinoma SW480 cells and in metastasis-derived SW620 cells. On the other hand, FXR gene expression increases with the degree of differentiation in the Caco-2 and HT-29 cell lines [26]. Thus, lesser expression of FXR seems to be associated with a more undifferentiated phenotype in breast and colon carcinomas.

In the whole group of breast cancers, significant correlations were observed between the expression of FXR and those of proliferation markers, including cyclin D and c-myc. These results are in agreement with a previous study which reports that FXR is highly expressed in a Barrett's esophagus-derived cell line and may influence cell survival [27]. Indeed, the FXR antagonist guggulsterone induces cell apoptosis through an effect attributed to the downregulation of cyclin D and c-myc [28]. Moreover, in the ER-positive subgroup of breast tumors, FXR expression was highly correlated with cyclin D and p27 protein expression. This result is in line with the fact that the expressions of both cyclin D1 and p27 are closely related [29, 30] and correlate with estrogen receptor positivity in primary breast cancer [31, 32]. Therefore, insofar as mitogen-dependent progression through G_1 phase is mediated by induction of the cyclin D family [33, 34], our study suggests that FXR expression is associated with cell proliferation.

On the other hand, no association was observed between FXR expression and neoplasm recurrence in the total population or in the ER-positive subgroup (data not shown). Interestingly, in good prognosis patients (no recurrence during 10 years of follow-up), FXR expression was correlated with several proliferation factors (cyclin D and p27), whereas in the poor outcome patients (distant metastasis), it was exclusively correlated with c-myc. Of note, c-myc and cyclin D1 participate in the activation of the cyclin E-cdk2 complexes by overriding the cell cycle

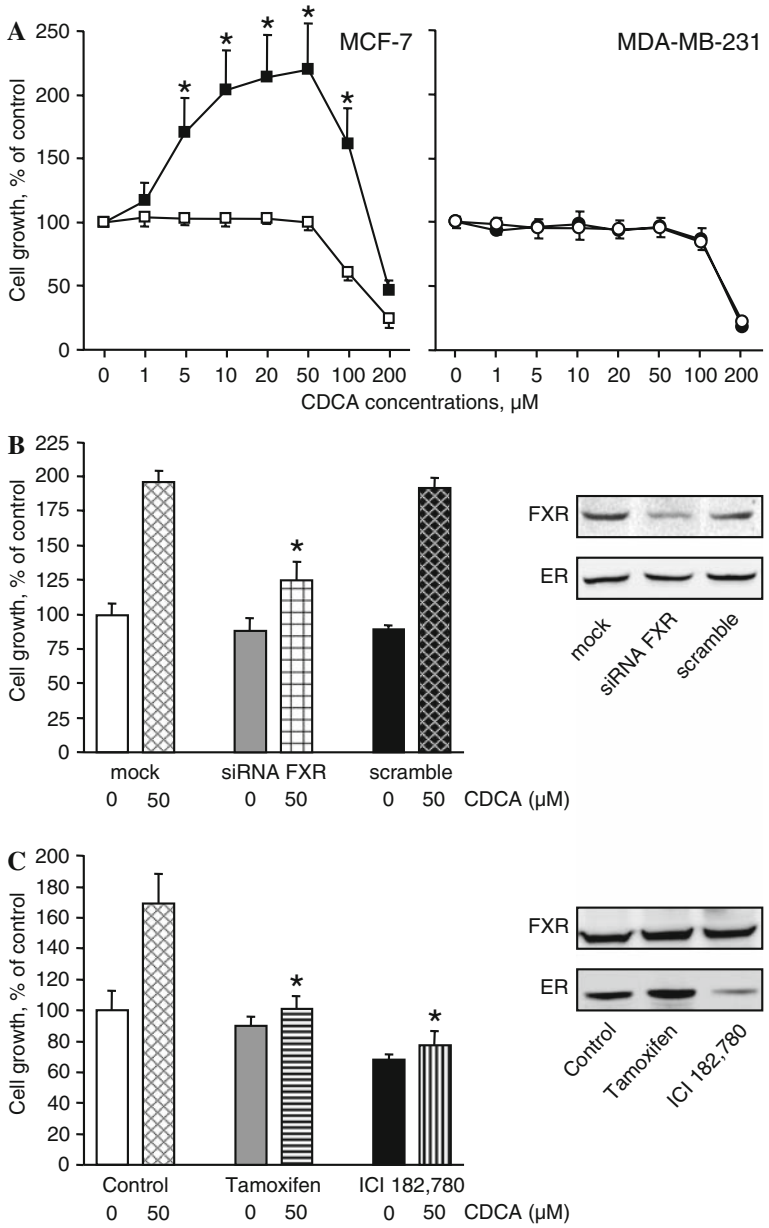

Fig. 3 Effects of CDCA on the proliferation of MCF-7 and MDA-MB-231 cells. (**a**) Breast cancer cells were treated for 72 h with 1–200 μM CDCA or vehicle in steroid-free medium (SFM) (filled symbols) or E_2-supplemented SFM (open symbol). Cell proliferation was determined by crystal violet staining assay. Data are presented as percentages of control values (mean ± SD). Mean of results pooled from 2 experiments ($n = 12$). * ANOVA, $P < 0.05$ vs. untreated cells. (**b**) Effect of FXR gene silencing on the mitogenic effect of CDCA in MCF-7 cells. Cancer cells were transfected for 6 h with 50 nM siRNA duplex against FXR, corresponding scramble (negative control), or vehicle (mock). Transfected cells were exposed to 50 μM CDCA or vehicle for 3 days before assessment of cell proliferation as described above. Mean of results pooled from 2 experiments ($n = 12$). * ANOVA, $P < 0.05$ vs. CDCA-treated cells (mock condition). In parallel, transfected cells were subjected to FXR and ER determinations (Western blot analysis). (**c**) Effect of antiestrogens on the growth stimulation induced by CDCA in MCF-7 cells. Tumor cells were exposed for 3 days to vehicle, 50 μM CDCA, 100 nM 4-hydroxytamoxifen (tamoxifen), and/or 100 nM fulvestrant (ICI 182,780). Cell growth was assessed as described above. Mean of results pooled from 2 experiments ($n = 12$). * ANOVA, $P < 0.05$ vs. CDCA-treated cells (control condition). Additionally, the effects of antiestrogens on FXR and ER expressions were examined by Western blot analysis

arrest imposed by p27 overexpression [35]. No definite conclusion can, however, be drawn since the number of patients with poor prognosis was low. Nevertheless, these data suggest that FXR expression could be associated with proliferation in ER-positive tumors through different mechanisms contributing to tumor aggressiveness.

Interestingly, the association between FXR expression and cell proliferation (Ki-67) was only noted in

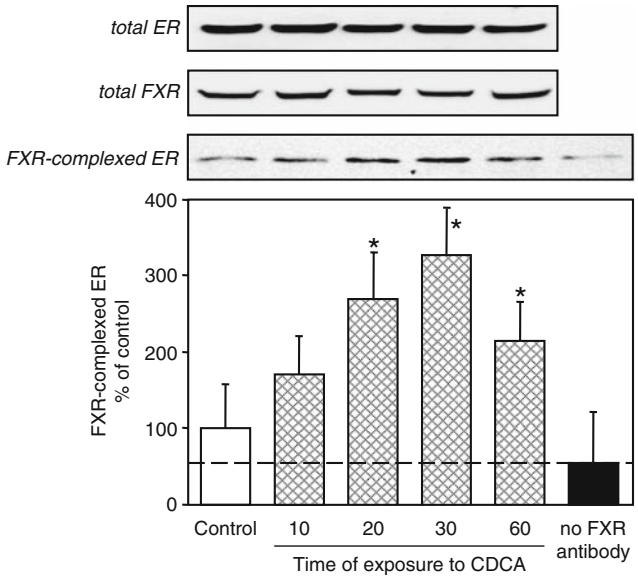

Fig. 4 Western blotting of ER in immunoprecipitated FXR preparations. MCF-7 cells were incubated in SFM with 50 μM CDCA or vehicle (control) for 10, 20, 30 or 60 min. Solubilized protein preparations were submitted to FXR immunoprecipitation, as described in "Material and Methods". ER expression was assayed in the immunoprecipitates by Western blotting. The second control "no FXR antibody" means that no primary antibody was used for immunoprecipitation. The broken line refers to the non specific signal level. Quantitative data were obtained from densitometric analyses ($n = 3$) and are presented as percentages of control values (mean ± SD). * ANOVA, $P < 0.05$ vs. control. Total ER and FXR levels were determined by Western blotting in cell extracts before immunoprecipitation

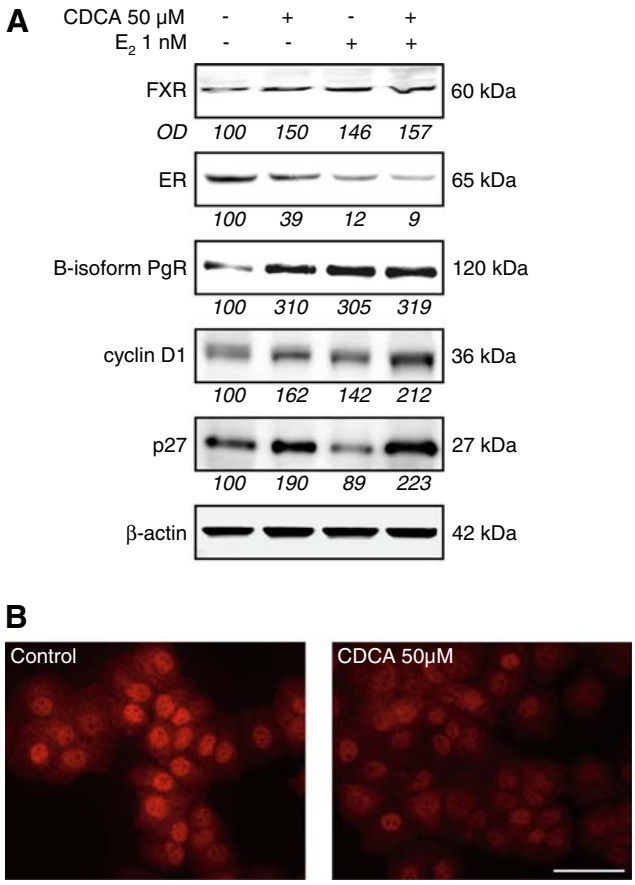

Fig. 5 Expression and regulation of FXR and biomarkers in MCF-7 cells exposed to CDCA and/or 17β-estradiol (E_2). (**a**) MCF-7 cells cultured in SFM were incubated for 24 h with 50 μM CDCA and/or 1 nM E_2, or vehicle. Equal quantities of proteins were submitted to 8, 10 or 12% SDS-PAGE (depending of the targeted proteins) and electrotransferred onto nitrocellulose membranes. Immunodetection was performed with a rabbit polyclonal anti-FXR/NR1H4 antibody, a mouse monoclonal anti-ERα antibody, a mouse monoclonal anti-PgR (A/B isoforms) antibody, a mouse monoclonal anti-cyclin D1 antibody, or a rabbit polyclonal anti-p27 antibody. β-actin was used as a loading control. Quantitative data were obtained from densitometric analyses ($n = 3$) and are presented as mean percentages. (**b**) ER demonstration by immunofluorescence microscopy. A rabbit polyclonal anti-ER antibody was used as the primary reagent. Texas Red labeling. Magnification bar: 10 μm

ER-positive tumors from postmenopausal patients. This observation is in agreement with our in vitro data, which indicate that FXR activation by chenodeoxycholic acid (CDCA) has no effect in breast cancer cell lines in estrogen-containing medium, while it stimulates the proliferation of the ER-positive cell line MCF-7 in steroid-free medium (an experimental condition mimicking low levels of circulating estrogens in postmenopausal women). As previously demonstrated for the FXR activator farnesol [15], CDCA might promote a positive crosstalk between FXR and ER, accounting for FXR-mediated ER activation in absence of estrogen stimulation and mitogenic response of ER-positive cells to this FXR agonist. It must be noted that the concentration of CDCA used in the current study (50 μM) is clinically relevant since it is in the range of those observed in human breast cyst fluid (42–94 μM) [18].

The correlation between FXR expression and tumor cell proliferation in postmenopausal patients could be extended to the clinical context of breast cancer patients treated with aromatase inhibitors. Indeed, the latter drugs markedly decrease plasma estrogen level by inhibiting or inactivating aromatase enzymes responsible for the synthesis of estrogens from androgenic substrates [36], and also strongly inhibit intratumoral aromatase activity present in the majority of breast cancers [37]. Thus, aromatase inhibitor treatments could disclose a possible crosstalk between FXR and ER, which may induce proliferative responses and lead to some forms of resistance to hormone therapy.

Bile acids, which are endogenous ligands/activators of FXR, have been implicated in the development of colorectal cancers [38]. Moreover, the involvement of FXR ligands in breast carcinogenesis has been previously documented. Indeed, high concentrations of plasma deoxycholate acid (DCA) are found in human breast cyst fluid from patients with fibrocystic disease of the breast and have been discussed

as risk factors for developing breast cancer [17, 18]. More recently, plasma bile acid concentrations were reported to be higher in postmenopausal women newly diagnosed with breast cancer, as compared to healthy controls matched for age and body mass index [16]. In addition, the current study reveals that chenodeoxycholic acid (CDCA) promotes the growth of MCF-7 cells. Altogether, these data further support the hypothesis that bile acids might play a role in the etiology of breast carcinoma [39].

Obesity in postmenopausal women increases the risk of developing breast cancer [40], and results in increased bile acid output [41]. Breast cancer incidence is epidemiologically linked to high-fat diets [42] which increase the amount of bile acids in the body [43]. Moreover, some studies indicate that high-fat diets are associated with increased risk for ER-positive breast tumors [44–46]. All of these data suggest that FXR activation by higher bile acid levels associated with obesity or high-fat diets might contribute to breast carcinogenesis.

Finally, a recent study indicates that the bile acid salt sodium deoxycholate (DC) may promote the survival and the migration of the metastatic MDA-MB-231 cell line through the induction of urokinase-type plasminogen activator, a critical factor for the dissemination of breast cancer cells [13]. These data suggest that, in addition to the involvement of FXR in cell survival/proliferation, this nuclear receptor could be involved in tumor invasiveness/metastasis, as further supported by the significant correlation between FXR expression and nodal status in our population. In this regard, we have found recently that FXR expression in primitive breast tumors appeared associated with the propensity for bone metastasis [47].

In conclusion, the current study suggests a close association between FXR and ER expression. Moreover, FXR expression was correlated with tumor proliferation only in ER-positive breast cancers in postmenopausal women. Therefore, FXR may prove to be a valuable biomarker to further characterize high and low proliferating tumors in ER-positive breast cancers, especially in estrogen deprived patients (postmenopause, treatment with aromatase inhibitors).

Acknowledgements This study received financial support from the "Fondation Medic", from the "Fondation contre le Cancer", from the Belgian Fund for Medical Scientific Research (grants no. 3.4512.03 and 3.4501.08), from the "Fondation Lambeau-Marteaux", and from "Les Amis de l'Institut Bordet". Virginie Durbecq, Christos Sotiriou and Guy Laurent are respectively Scientific Research Worker, Research Associate and Senior Research Associate of the National Fund for Scientific Research (Belgium).

References

1. Forman BM, Goode E, Chen J, Oro AE, Bradley DJ, Perlmann T, Noonan DJ, Burka LT, McMorris T, Lamph WW et al (1995) Identification of a nuclear receptor that is activated by farnesol metabolites. Cell 81:687–693
2. Wang H, Chen J, Hollister K, Sowers LC, Forman BM (1999) Endogenous bile acids are ligands for the nuclear receptor FXR/BAR. Mol Cell 3:543–553
3. Makishima M, Okamoto AY, Repa JJ, Tu H, Learned RM, Luk A, Hull MV, Lustig KD, Mangelsdorf DJ, Shan B (1999) Identification of a nuclear receptor for bile acids. Science 284:1362–1365
4. Parks DJ, Blanchard SG, Bledsoe RK, Chandra G, Consler TG, Kliewer SA, Stimmel JB, Willson TM, Zavacki AM, Moore DD et al (1999) Bile acids: natural ligands for an orphan nuclear receptor. Science 284:1365–1368
5. Modica S, Moschetta A (2006) Nuclear bile acid receptor FXR as pharmacological target: are we there yet? FEBS Lett 580:5492–5499
6. Lee FY, Lee H, Hubbert ML, Edwards PA, Zhang Y (2006) FXR, a multipurpose nuclear receptor. Trends Biochem Sci 31:572–580
7. Edwards PA, Kast HR, Anisfeld AM (2002) BAREing it all: the adoption of LXR and FXR and their roles in lipid homeostasis. J Lipid Res 43:2–12
8. Kalaany NY, Mangelsdorf DJ (2006) LXRS and FXR: the yin and yang of cholesterol and fat metabolism. Annu Rev Physiol 68:159–191
9. Claudel T, Sturm E, Kuipers F, Staels B (2004) The farnesoid X receptor: a novel drug target? Expert Opin Investig Drugs 13:1135–1148
10. Westin S, Heyman RA, Martin R (2005) FXR, a therapeutic target for bile acid and lipid disorders. Mini Rev Med Chem 5:719–727
11. Bishop-Bailey D, Walsh DT, Warner TD (2004) Expression and activation of the farnesoid X receptor in the vasculature. Proc Natl Acad Sci USA 101:3668–3673
12. He F, Li J, Mu Y, Kuruba R, Ma Z, Wilson A, Alber S, Jiang Y, Stevens T, Watkins S et al (2006) Downregulation of endothelin-1 by farnesoid X receptor in vascular endothelial cells. Circ Res 98:192–199
13. Silva J, Dasgupta S, Wang G, Krishnamurthy K, Ritter E, Bieberich E (2006) Lipids isolated from bone induce the migration of human breast cancer cells. J Lipid Res 47:724–733
14. Swales KE, Korbonits M, Carpenter R, Walsh DT, Warner TD, Bishop-Bailey D (2006) The farnesoid X receptor is expressed in breast cancer and regulates apoptosis and aromatase expression. Cancer Res 66:10120–10126
15. Journe F, Laurent G, Chaboteaux C, Nonclercq D, Durbecq V, Larsimont D, Body JJ (2008) Farnesol, a mevalonate pathway intermediate, stimulates MCF-7 breast cancer cell growth through farnesoid-X-receptor-mediated estrogen receptor activation. Breast Cancer Res Treat 107:49–61
16. Costarelli V, Sanders TA (2002) Plasma deoxycholic acid concentration is elevated in postmenopausal women with newly diagnosed breast cancer. Eur J Clin Nutr 56:925–927
17. Raju U, Levitz M, Javitt NB (1990) Bile acids in human breast cyst fluid: the identification of lithocholic acid. J Clin Endocrinol Metab 70:1030–1034
18. Javitt NB, Budai K, Miller DG, Cahan AC, Raju U, Levitz M (1994) Breast-gut connection: origin of chenodeoxycholic acid in breast cyst fluid. Lancet 343:633–635
19. Costarelli V, Sanders TA (2002) Plasma bile acids and risk of breast cancer. IARC Sci Publ 156:305–306
20. McShane LM, Altman DG, Sauerbrei W, Taube SE, Gion M, Clark GM (2006) REporting recommendations for tumor MARKer prognostic studies (REMARK). Breast Cancer Res Treat 100:229–235
21. Allred DC, Harvey JM, Berardo M, Clark GM (1998) Prognostic and predictive factors in breast cancer by immunohistochemical analysis. Mod Pathol 11:155–168

22. Colozza M, Azambuja E, Cardoso F, Sotiriou C, Larsimont D, Piccart MJ (2005) Proliferative markers as prognostic and predictive tools in early breast cancer: where are we now? Ann Oncol 16:1723–1739
23. Prall OW, Sarcevic B, Musgrove EA, Watts CK, Sutherland RL (1997) Estrogen-induced activation of Cdk4 and Cdk2 during G1-S phase progression is accompanied by increased cyclin D1 expression and decreased cyclin-dependent kinase inhibitor association with cyclin E-Cdk2. J Biol Chem 272:10882–10894
24. Foster JS, Henley DC, Bukovsky A, Seth P, Wimalasena J (2001) Multifaceted regulation of cell cycle progression by estrogen: regulation of Cdk inhibitors and Cdc25A independent of cyclin D1-Cdk4 function. Mol Cell Biol 21:794–810
25. Sherr CJ, Roberts JM (1995) Inhibitors of mammalian G1 cyclin-dependent kinases. Genes Dev 9:1149–1163
26. De Gottardi A, Touri F, Maurer CA, Perez A, Maurhofer O, Ventre G, Bentzen CL, Niesor EJ, Dufour JF (2004) The bile acid nuclear receptor FXR and the bile acid binding protein IBABP are differently expressed in colon cancer. Dig Dis Sci 49:982–989
27. De Gottardi A, Dumonceau JM, Bruttin F, Vonlaufen A, Morard I, Spahr L, Rubbia-Brandt L, Frossard JL, Dinjens WN, Rabinovitch PS et al (2006) Expression of the bile acid receptor FXR in Barrett's esophagus and enhancement of apoptosis by guggulsterone in vitro. Mol Cancer 5:48
28. Shishodia S, Aggarwal BB (2004) Guggulsterone inhibits NF-kappaB and IkappaBalpha kinase activation, suppresses expression of anti-apoptotic gene products, and enhances apoptosis. J Biol Chem 279:47148–47158
29. Fredersdorf S, Burns J, Milne AM, Packham G, Fallis L, Gillett CE, Royds JA, Peston D, Hall PA, Hanby AM et al (1997) High level expression of p27(kip1) and cyclin D1 in some human breast cancer cells: inverse correlation between the expression of p27(kip1) and degree of malignancy in human breast and colorectal cancers. Proc Natl Acad Sci USA 94:6380–6385
30. Sweeney KJ, Swarbrick A, Sutherland RL, Musgrove EA (1998) Lack of relationship between CDK activity and G1 cyclin expression in breast cancer cells. Oncogene 16:2865–2878
31. Hui R, Cornish AL, McClelland RA, Robertson JF, Blamey RW, Musgrove EA, Nicholson RI, Sutherland RL (1996) Cyclin D1 and estrogen receptor messenger RNA levels are positively correlated in primary breast cancer. Clin Cancer Res 2:923–928
32. Catzavelos C, Bhattacharya N, Ung YC, Wilson JA, Roncari L, Sandhu C, Shaw P, Yeger H, Morava-Protzner I, Kapusta L et al (1997) Decreased levels of the cell-cycle inhibitor p27Kip1 protein: prognostic implications in primary breast cancer. Nat Med 3:227–230
33. Sherr CJ (1996) Cancer cell cycles. Science 274:1672–1677
34. Sherr CJ, Roberts JM (1999) CDK inhibitors: positive and negative regulators of G1-phase progression. Genes Dev 13: 1501–1512
35. Mateyak MK, Obaya AJ, Sedivy JM (1999) c-Myc regulates cyclin D-Cdk4 and -Cdk6 activity but affects cell cycle progression at multiple independent points. Mol Cell Biol 19:4672–4683
36. Brodie AM, Njar VC (2000) Aromatase inhibitors and their application in breast cancer treatment*. Steroids 65:171–179
37. Blankenstein MA, van de Ven J, Maitimu-Smeele I, Donker GH, de Jong PC, Daroszewski J, Szymczak J, Milewicz A, Thijssen JH (1999) Intratumoral levels of estrogens in breast cancer. J Steroid Biochem Mol Biol 69:293–297
38. Nagengast FM, Grubben MJ, van Munster IP (1995) Role of bile acids in colorectal carcinogenesis. Eur J Cancer 31A:1067–1070
39. Lewis SJ, Heaton KW (1999) The metabolic consequences of slow colonic transit. Am J Gastroenterol 94:2010–2016
40. Carmichael AR (2006) Obesity as a risk factor for development and poor prognosis of breast cancer. BJOG 113:1160–1166
41. Halmy L, Feher T, Steczek K, Farkas A (1986) High serum bile acid level in obesity: its decrease during and after total fasting. Acta Med Hung 43:55–58
42. Cho E, Spiegelman D, Hunter DJ, Chen WY, Stampfer MJ, Colditz GA, Willett WC (2003) Premenopausal fat intake and risk of breast cancer. J Natl Cancer Inst 95:1079–1085
43. Costarelli V, Sanders TA (2001) Acute effects of dietary fat composition on postprandial plasma bile acid and cholecystokinin concentrations in healthy premenopausal women. Br J Nutr 86:471–477
44. Harlan LC, Coates RJ, Block G, Greenberg RS, Ershow A, Forman M, Austin DF, Chen V, Heymsfield SB (1993) Estrogen receptor status and dietary intakes in breast cancer patients. Epidemiology 4:25–31
45. Kushi LH, Potter JD, Bostick RM, Drinkard CR, Sellers TA, Gapstur SM, Cerhan JR, Folsom AR (1995) Dietary fat and risk of breast cancer according to hormone receptor status. Cancer Epidemiol Biomarkers Prev 4:11–19
46. Jain M, Miller AB (1997) Tumor characteristics and survival of breast cancer patients in relation to premorbid diet and body size. Breast Cancer Res Treat 42:43–55
47. Journe F, Durbecq V, Chaboteaux C, Rouas G, IdBoufker H, Laurent G, Larsimont D, Body J (2008) Farnesoid X receptor in primary breast carcinoma: a new marker to predict bone metastasis? Bone 42(Suppl 1):S97 (abstract 175)